Sensors and Materials, Vol. 34, No. 6 (2022) 2447–2466
MYU Tokyo

S & M 2982

Coolant Volume Prediction for Spindle Cooler with Adaptive Neuro-fuzzy Inference System Control Method

Ming-Chu Hsieh,[1] Swami Nath Maurya,[2] Win-Jet Luo,[2*]
Kun-Ying Li,[2] Li Hao,[1] and Prakash Bhuyar[3]

[1]Department of Mechanical Engineering, National Chin-Yi University of Technology,
No. 57, Sec. 2, Zhongshan Rd., Taiping Dist., Taichung 41170, Taiwan
[2]Graduate Institute of Precision Manufacturing, National Chin-Yi University of Technology,
No. 57, Sec. 2, Zhongshan Rd., Taiping Dist., Taichung 41170, Taiwan
[3]Energy Research Centre (ERC), International College, Maejo University,
No. 63 Moo 4, Nong Han Subdistrict, San Sai District, Chiang Mai Province 50290, Thailand

(Received December 29, 2021; accepted June 1, 2022)

Keywords: adaptive neuro-fuzzy inference system (ANFIS), machine tool, spindle cooling, thermal deformation, thermal suppression

Machining dynamics plays an essential role in machine tools (MTs) and machining operations, directly impacting the material removal rate, surface quality, and dimensional accuracy. With the increasing use of numerical control (NC) MTs and increasing automation of production, machining inaccuracy due to thermal deformation has become a significant issue. Furthermore, since the rotation speed and feed rate have risen, more heat is produced in MTs. In addition, since high machining precision is now required, techniques to avoid or regulate thermal deformation are also needed. Traditionally, researchers used the finite element method, support vector method (SVM), regression analysis method, neural network, and other methods to predict and compensate for the thermal deformation of MT spindles. However, these methods do not directly reduce the thermal errors caused by the heat source to improve the accuracy of MTs. Therefore, in this study, a cooling control method is proposed to reduce the impact of heat on the spindle by using a thermal suppression technique accompanied by the adaptive neuro-fuzzy inference system (ANFIS) control method to predict the static thermal behavior of a spindle. The root mean square error (RMSE) is used as the ANFIS evaluation index to reflect the quality of the prediction model. This method is implemented in Simulink to simulate the dynamics of the coolant during the real-time monitoring of the cutting and resting positions of the MT. Finally, a thermal deformation prediction model is generated to demonstrate that the cooling control method developed in this study can be applied to the intelligent cooling of an MT. It is shown that the developed ANFIS prediction model is efficient for controlling cooling. A simulation also shows that this method can reduce the running cost, energy consumption and accurately predict the thermal deformation of MT spindles. It is predicted that the most suitable coolant pump operating frequencies for the spindle at rotation speeds of 2000, 8000, 10000, and 12000 rpm are 20, 40, 40, and 60 Hz and the reductions of the spindle heat are 92.4, 99.9, 80.1, and 60.2%, respectively, with a prediction accuracy within 4.745 μm.

*Corresponding author: e-mail: : wjluo@ncut.edu.tw
https://doi.org/10.18494/SAM3794

ISSN 0914-4935

1. Introduction

High-speed automatic processing is necessary for manufacturing mechanical products with high processing precision and an even surface. Therefore, it has been widely applied in many equipment manufacturing industries, and high-speed machine tools (MTs) have become essential in the equipment manufacturing industry. A motorized spindle is the main component of current MT technology and the main conveyor for high-speed cutting technology.[1] Thermal phenomena cause most machining defects in MTs, and their reduction substantially improves the efficiency of machining operations. As the requirement for machining precision rises, it becomes increasingly essential to reduce thermal errors. The behavior of an MT in operation is affected by thermal errors, which are influenced by the intensity of the heat source. Thermal errors can be reduced by installing a cooling system in the MT spindle and improving the cooling channel design.[2–4] Two coolant control methods are often adopted in cooling systems: the varied coolant volume (VOV) control method and the constant coolant volume (COV) control method.[5] Using the VOV control method rather than the COV control method allows fine-tuning of the coolant circulating flow rate in terms of the machining load and spindle rotation speed to remove heat generated in the MTs, particularly internal heat generated by the spindle. The thermal deformation can be significantly reduced in the *Y*- and *Z*-directions by 70.1 and 73.5%, respectively, by applying the VOV control method.[6]

Grama *et al.*[7] found that the cooling effect is dramatically enhanced using a cooler trigger model (CTM)-based control technique on a conventional bath recirculation cooler unit. This technique involves dynamically controlling the switching frequency and the cooler compressor switch 'ON' time so that the heat exchange is according to the cooling load. The resulting thermal distortion using the CTM is significantly reduced compared with that of the conventional ambient temperature tracing strategy (ATS). For instance, the average error reductions are 51.2 and 47.6% for thermal expansion, 51.4% and 50% for the pitch angle, and 27.2 and 23.5% for the yaw angle for the CTM and ATS, respectively. Liu *et al.*[8] introduced a differentiated multiloop bath recirculation system that can accomplish the differentiated and close-loop cooling strategies in different heat-generating parts of precision MTs. Compared with a traditional bath recirculation cooler, it is more flexible and advantageous in controlling the temperature field and thermal error of precision MTs. Zhang *et al.*[9] proposed an active coolant technique for spindle thermal balance control to accurately dissipate disturbing heat transfers. The relationship among spindle internal heat generation, external heat convection, and coolant heat dissipation has been established analytically. The proposed active coolant strategy is more suitable than the previous power-matching techniques for an MT with a temperature-time variance (about 3.5 °C). The reductions of the spindle thermal error in the *X*-, *Y*-, and *Z*-directions were 92.9, 31.5, and 53.7%, respectively. Chiang *et al.*[10] developed a novel temperature control scheme by combining the proportional integral derivative (PID) controller with the Smith predictive method to precisely control the nonlinear and time-varying problems with time delay characteristics. They controlled the accuracy of the coolant outlet temperature at 0.1 °C and also effectively improved the performance of the traditional PID controller by using a hot-gas bypass valve. Mori *et al.*[11] studied the ON–OFF switch cooling control method to make a refrigeration system stop supplying coolant during the stop phase. There was no need to circulate the coolant, reducing

unnecessary power consumption and heat generation during this phase. They found that a time interval of 2 min is ideal for cooling the condenser to avoid switching the cooling device too frequently and reducing its life. This method can reduce the power consumption of the refrigeration system by as much as 75%.

MT software and hardware programming control technologies have been developed over many years to achieve high precision and versatility. However, most cutting procedures are still manually compiled by computers that automatically carry out numerical control (NC). Innovative technological breakthroughs are needed in software and hardware to achieve intelligent MTs. For example, a characteristic of intelligent MTs is reasonable ability at learning with a logical understanding and thinking mode. Appropriate decisions are automatically made for intelligent MTs to solve various problems in cutting processes; there is no need to instruct the MT while operating through additional NC commands.

The adaptive neuro-fuzzy inference system (ANFIS) introduced by Jang in 1993 is a prominent neuro-fuzzy system. ANFIS incorporates neural network and fuzzy logic components, the former capitalizing on the capacity to learn and the ability to generalize. Logical reasoning based on inference rules is derived from fuzzy logic, resulting in an instrument that can work with linguistic variables and incorporate a broad range of approaches.[12] Toward realizing intelligent MTs, Keshwani *et al.*[13] applied fuzzy prediction models to predict the permeability of compounds through the skin under various conditions. In their study, leave-one-out cross-validation (LOOCV) was combined with the root mean square error (RMSE) and coefficient of determination (R^2) to evaluate the model performance, which was compared with the regression model. It was found that the prediction performance of the fuzzy model is better than that of the regression model. The fuzzy model was used to quickly determine an initial estimate of the skin permeability coefficient to determine the transdermal drug delivery and toxicity potential. Al-Mahasneh *et al.*[14] used ANFIS in food processing technology. They applied it to the prediction of microbial growth, thermal process modeling, food quality control, and food rheology, including food drying and the analysis of food characteristics. They compared ANFIS with other modeling methods, such as an artificial neural network (ANN), support vector method (SVM), and multiple linear regression (MRA), and they found that ANFIS had significantly higher performance than these methods.

Sonmez *et al.*[15] developed an ANFIS model to predict the cadmium (Cd) concentration in the Filios river in Turkey. The developed model used the fewest possible number of parameters to calculate the Cd concentration. They found a high correlation coefficient ($R^2 = 0.91$) between observed and modeled Cd concentrations, showing that the ANFIS model is a reliable approach for predicting the concentration of Cd in water resources. Because of the reliability and accuracy of the ANFIS model, it is used to predict the concentration of heavy metals in water resources. For empirical forecasting systems, ANFIS is highly recommended as a processing method. Bensaber *et al.*[16] developed a model based on ANFIS for predicting the security index of an ad hoc vehicular network. The ANFIS system is computationally efficient, and one of its most advantageous features is that when one of the system parameters changes suddenly, the system improves its dynamic performance and has excellent stability. The predictive model shows that, by using the ANFIS method, a security index can be obtained to predict the possibility of attack and the effectiveness of protection.

Akkaya[17] developed an ANFIS model for predicting the higher heating value (HHV) of biomass. The input dataset for the prediction model consisted of proximate analysis components such as fixed carbon, ash, and volatile matter. Three methods are used in the construction of the ANFIS model, grid partition (GP), sub-clustering, and fuzzy c-means (FCM), to create a fuzzy inference system (FIS). Several simulation experiments were conducted for each FIS technique to determine the optimum ANFIS-based prediction model. It was found that the ANFIS model based on sub-clustering was the most accurate biomass HHV prediction model. In the testing phase, the resulting regression coefficient (R^2) and RMSE were 0.8836 and 1.3006, respectively, showing that the developed ANFIS model effectively predicts biomass HHV with high accuracy. Abdulshahed *et al.*[18] developed thermal error modeling based on ANFIS to establish the correlation between thermal errors and temperature changes. They considered two different ANFIS models: GP and FCM clustering. They used a computer numerical control (CNC) milling machine to build and test both models. The ANFIS-FCM model gave superior results with a maximum residual error of ±4 μm and a 94% reduction in the error.

Researchers currently use different thermal compensation technologies to reduce the thermal errors caused by MTs, but thermal errors cannot be removed effectively. Computer control calculations are performed for the thermal compensation of MTs, but there is no solution for heat reduction. However, in this study, we use VOV thermal suppression rather than thermal compensation as a cooling method to reduce the heat generation of an MT spindle. The main principle of this method is to adjust the coolant pump operating frequency and control the coolant volume according to the machining load to reduce the thermal deformation of MTs. If the heat generation is relatively high, then the coolant pump frequency will be high, which increases the coolant volume; similarly, if the heat generation is low, the coolant pump frequency will be low, which decreases the coolant volume.

In this study, the operating frequency control of the coolant pump is used as a predictive tool. To make the system closer to control based on human judgment, the optimal coolant pump frequency of the cooling system is used to obtain the best advice of the forecasting system. The control system can also adjust the power according to changes in the spindle's thermal state to reduce the energy consumption of the system.

2. Materials and Methods

2.1 Development method

ANFIS is an adaptive network that comprises input-output variables and a Takagi–Sugeno-type fuzzy rule. It is an adaptive and multilayer feed-forward network. For simplicity, the ANFIS framework is considered to have two inputs, x and y, and one output, z. Then, given a first-order Takagi–Sugeno fuzzy model, an appropriate rule set with two fuzzy if-then rules may be written as Eq. (1). Linguistic variables are used to assess entries (C_1, D_1). The outcome of each rule is obtained by combining the input values with a constant term (r_1).

$$\begin{aligned} &\text{Rule 1: If } x \text{ is } C_1 \text{ and } y \text{ is } D_1, \text{ then } z_1 = p_1 x + q_1 y + r_1 \\ &\text{Rule 2: If } x \text{ is } C_2 \text{ and } y \text{ is } D_2, \text{ then } z_2 = p_2 x + q_2 y + r_2 \end{aligned} \tag{1}$$

The functionality of each layer is discussed as follows and shown in Fig. 1:[18–21]

Layer 1: The primary function of this layer is to map input variables (x and y) into fuzzy sets $A = \{C_1, C_2, D_1, D_2\}$ through the process of fuzzification. Each node in this layer is square with functions for generating membership grades. C and D are linguistic labels (such as "low" and "high") characterized by different membership functions such as a generalized bell, sigmoid, or triangular function.

Layer 2: This layer uses the activation strength after integrating each input fuzzy set. The Π-norm operator performing the fuzzy conjunction ("and") is used to obtain the output.

Layer 3: The main task of this layer is to calculate the ith rule ratio of the activation strength to the sum of all activation strengths.

Layer 4: In this layer, the output from the previous layer is multiplied by the Sugeno fuzzy rule function.

Layer 5: There is only one node in this layer. This node computes the sum of all outputs of each rule from the previous layer. Then, a weighted average method performs defuzzification, which transforms the fuzzy result into a crisp output.

2.2 Development of control system

The control method developed in this study involves the following steps:

Step 1: Temperature sensors (PT100 type, with measurement temperature ranging from −40 to +120 ºC) are mounted at the inlet and outlet of the coolant supply to measure the inlet and outlet coolants temperatures, respectively. A T-type sensor that can measure temperatures ranging from −250 to 370 ºC is used to measure the ambient temperature, and a displacement sensor (eddy current, AEC-S06) is mounted on the MT to measure the thermal deformation in the Z-direction based on the ISO 230-3 standard.

Step 2: Excel is used to organize and record the measured data, including the experimental parameters of each rotation speed.

Step 3: After sorting and organizing the data collected by the sensors into Excel, the data with R^2 higher than 0.68 is imported into MATLAB for the predictive modeling of the control system of the ANFIS cooling control method.

Step 4: To generate the FIS in ANFIS, this step is divided into three parts: setting, modification, and testing.

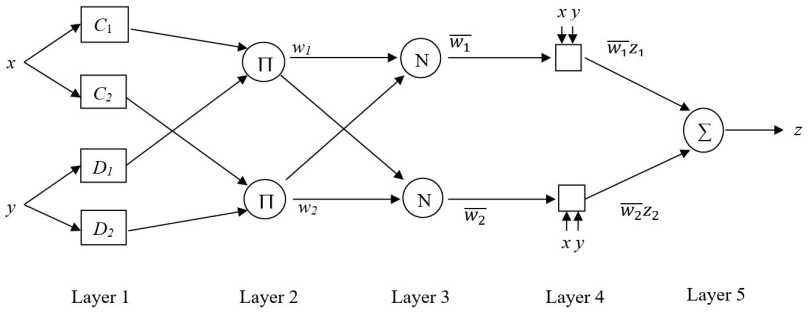

Fig. 1. ANFIS structure.

1. The operational interface for making FIS is entered, and the input and output parameters are selected and imported into the model training database.
2. The parameters of the inference system and the network learning method are adjusted.
3. After the predictive model of the coolant volume is developed by ANFIS, the predictive evaluation index (RMSE) is used to judge the accuracy of the developed model. If it does not meet the expected results, the three parts this step are repeated.

Step 5: In Simulink, a set of programs that can be used to simulate the actual operation of the MT for the predictive modeling using the cooling control methods are written to simulate the expected action of the main spindle of the MT as a function of the operating frequency of the coolant pump during operation.

Step 6: The analog control system infers and predicts the corresponding coolant pump operating frequency and then decompiles it into a reference value to find the coolant pump frequency of the main spindle in operation that can produce the greatest temperature suppression effect and the optimal spindle displacement conditions.

Step 7: The reference value corresponding to the predicted operating frequency of the coolant pump from the steady-state interval database is found.

Figure 2 shows the flow chart of the prediction model development and the operation of the control system.

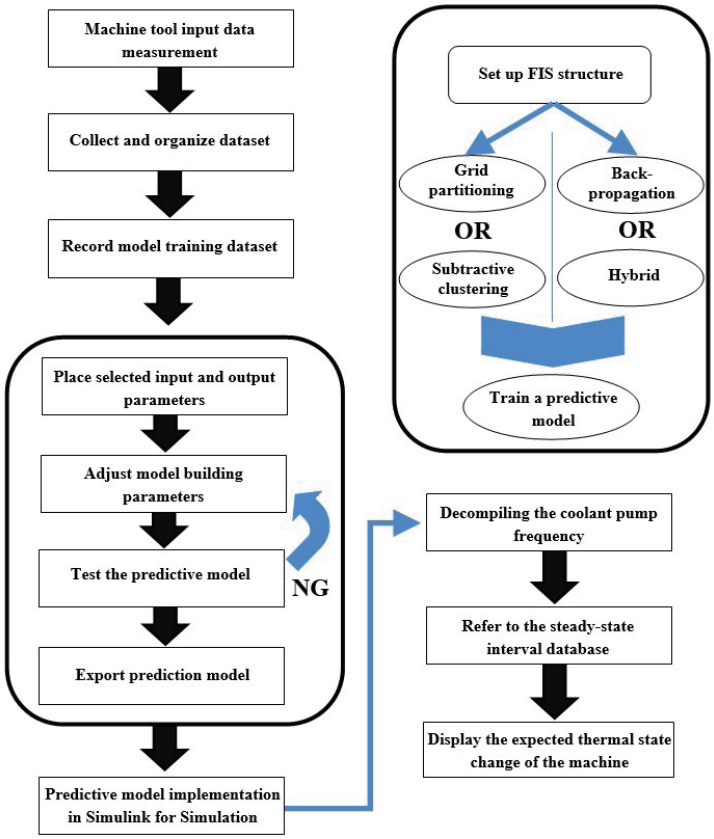

Fig. 2. (Color online) Flow chart of the prediction model development and the operation of the control system.

2.3 MT parameter selection

The modeling data used in this study is based on the measured data, and the thermal error measurement of MTs refers to the ISO 230–3 international standard. Note that this standard only deals with non-cutting or air cutting, different from the actual cutting condition (real cutting).

The dataset used in this study is based on the data measured and recorded during an experiment to analyze the steady-state time of a variable-frequency and fixed-frequency cooler. The dataset originates from the relevant measurement information of the MT recorded by the data recorder. The measurement data recorded in this experiment are listed in Table 1.

We selected the thermal deformation in the Z-direction, inlet coolant temperature, outlet coolant temperature, air temperature, temperature difference between the inlet and outlet coolants, coolant pump frequency, and spindle speed as modeling parameters.

The method uses a specific coolant pump frequency and targets a specific spindle speed. The coolant pump frequencies considered in the measurements are 0, 20, 40, 60, and 80 Hz and the spindle speeds are 2000, 8000, 10000, and 12000 rpm. The spindle state is measured at a fixed speed and coolant pump frequency. Each measurement is for 2 h. In the experiment, an interval of 1 h is assigned for machine cooling. Nine sets of measurement data are collected for each rotation speed, and each set of measurement data comprises about 35000 values. The dataset is used as an application and manually pre-organized with Excel to facilitate the construction of the forecasting model. The following methods and steps are used to process the Excel data:

Step 1: Divide the data for a single speed into groups of 0, 20, 40, 60, and 80 Hz.

Step 2: Use the data in each frequency group to record the *Z*-direction deformation, inlet coolant temperature, outlet coolant temperature, air temperature, temperature difference between the inlet and outlet coolants, and so forth, as reference data for the prediction model.

Step 3: Reduce the number of digits of the above data types.

Step 4: In the sorting of the data, use different data as a sorting benchmark.

Step 5: Since 19 data per second are entered into the recorder, a considerable amount of repeated data is generated, which must be reduced to avoid the burden of constructing the predictive model.

Step 6: Delete duplicate data.

Step 7: Repeat steps 4 to 6 until all duplicate data are deleted.

Table 1
Types of measurement data.

Measured item	Representation	Unit
Thermal deformation in Z-direction	Z_d	μm
Inlet coolant temperature	T_i	℃
Outlet coolant temperature	T_o	℃
Air temperature	T_{air}	℃
Front bearing temperature	T_{fb}	℃
Back bearing temperature	T_{bb}	℃
Temperature difference between inlet and outlet coolants	T_d	℃
Coolant pump frequency	*Freq*	Hz
Spindle speed	*Rpm*	rpm

The digits of displacement- and temperature-related data are adjusted to two decimal places. After reducing the number of digits of all speed groups, we found that there are tens of thousands of repeated data in each group. If the repeated data are included in the model construction, the system will crash during the construction period. On this basis, we reviewed the data obtained at 2000, 8000, 10000, and 12000 rpm and used them at each rotation speed. One FIS is used for each rotation speed; thus, four FISs with different spindle rotation speeds are used. In each FIS, the *Z*-direction deformation, inlet coolant temperature, outlet coolant temperature, air temperature, and coolant temperature difference are used as the model learning data, which are used to distinguish the system from the data.

From the simplified data of each FIS, 80% of the total data is used to train the model and the remaining 20% is used to test the fuzzy inference model. The above-divided dataset cannot be repeated to prevent the prediction model in the control system from inaccurate prediction. The divided data are used in the prediction modeling, including the thermal deformation in the *Z*-direction, inlet coolant temperature, outlet coolant temperature, air temperature, temperature difference between inlet and outlet coolants, and coolant pump frequency. The architecture of the FIS is shown in Fig. 3.

Each rotation speed has its own recorded data used as a predictive model. Considering the 2000 rpm dataset as an example, 80% of the data is divided into five frequencies used as model training data and 20% of the data is divided into five frequencies to verify and inspect the model. The above steps can generate a set of FISs. Then, the prediction system with analog control generates four groups, once for each rotation speed, namely, 2000, 8000, 10000, and 12000 rpm FIS, which are input to the corresponding signal after the pre-identification signal of the analog control system. The structure of the identified speed signal is shown in Fig. 4.

2.4 Predictive modeling

In this study, MATLAB R2019b is used as a fuzzy logic toolbox for a model-building tool. MATLAB provides three methods to create the initial FIS structure: GP, FCM clustering, and subtractive clustering (SC). In this study, the GP and SC methods are used to control the main structure of the FIS, then the ANFIS toolbox is used to input the relevant parameters into the software so that ANFIS can build a predictive model.

Figure 5(a) shows the homepage interface of the inference system of the fuzzy logic toolbox and the Sugeno-type inference system. The software provides Mamdani-type and Sugeno-type

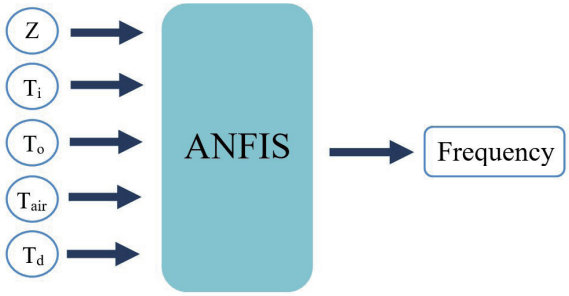

Fig. 3. (Color online) Architecture of the FIS.

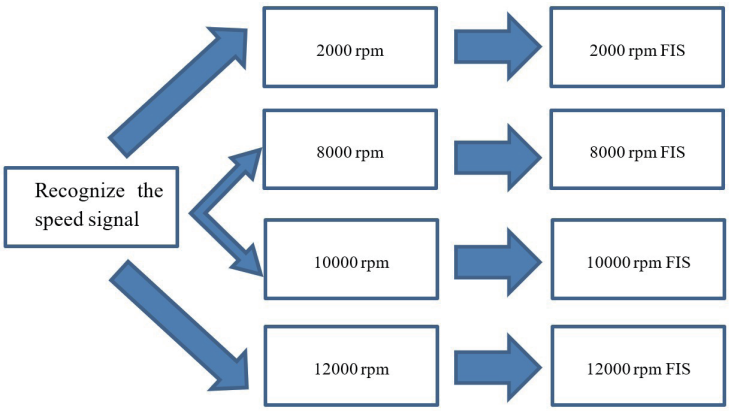

Fig. 4. (Color online) Structure of the identified speed signal.

inference methods for users. To use ANFIS as an application, the inference system must choose the Sugeno type as the architecture of the inference system. The interface can increase or decrease the input value and can adjust the name of each input and output, the method of the Boolean logic operation, the set relationship, the method of defuzzification, and other functions.

Figure 5(b) shows the detailed parameter-setting interface of each membership function. On this interface, we can adjust the range of each membership function, the name of the membership function, the display range, the extreme value of each membership function, and the value of each membership function.

Figure 6(a) shows the main operating interface of ANFIS modeling, in which training, testing, and verification data must be placed. The dataset shown in the right half of the image is placed in ANFIS for model training, testing, and verification. Regardless of the number of inputs, the last column must be the model's output. The GP and SC methods mentioned above can also be revised from this interface. There are two learning algorithms: the hybrid and backpropagation (BP) methods. The learning error tolerance can also be adjusted to avoid excessive coupling and reduction of the model accuracy. After the above parameter input is modified, the number of iterations can be modified for model training, and model accuracy can be verified after generation.

Figure 6(b) shows the fuzzy rules generated by the inference system after data training and learning. According to the current project, the user parameters can be further modified after modeling.

When using the GP method as the structure of the FIS, the user can customize the number of membership functions of the input value. The system generates rules by enumerating all possible combinations of the input membership functions and directly modifying them to meet the requirements. Suppose the suitable number of rules is known at the beginning. In that case, we can even enter the membership function corresponding to the number of inputs or further modify the appropriate membership function graph to increase its accuracy for data analysis and implementation of the GP method.

After repeated corrections and modeling, the relevant scoring index of the prediction model can be obtained. For example, the RMSE values of the three average-testing errors (ATEs) can

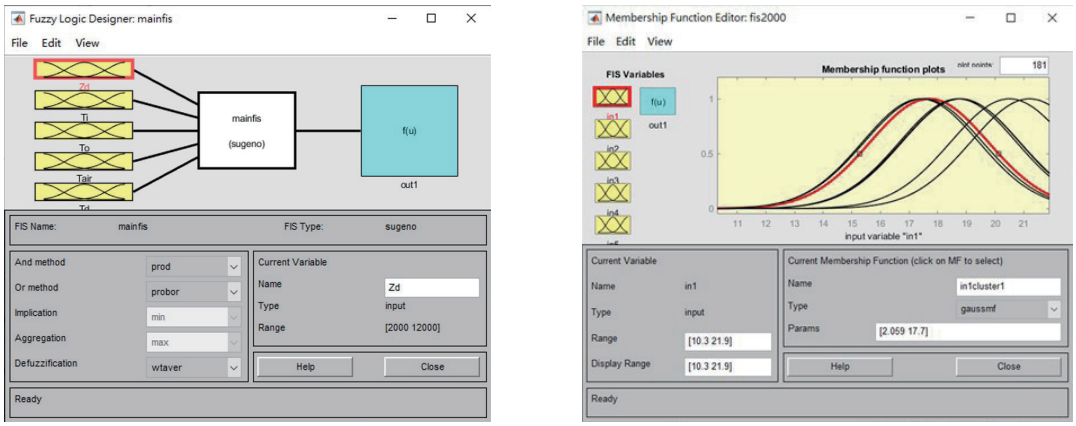

(a) (b)

Fig. 5. (Color online) (a) Sugeno-type inference system of fuzzy logic toolbox and (b) interface for setting membership function.

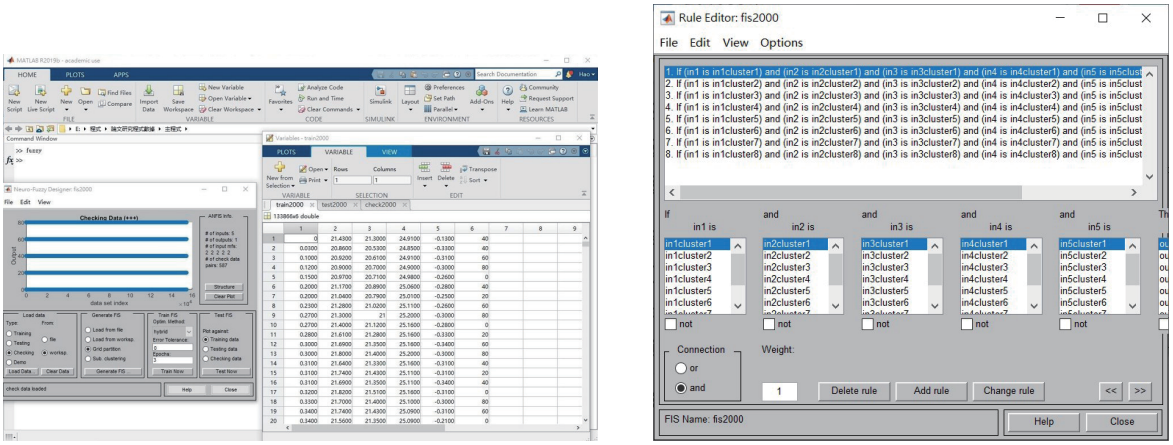

(a) (b)

Fig. 6. (Color online) (a) ANFIS modeling interface and (b) fuzzy logic rule database.

be lower than the RMSE of this modeling, which means that the prediction model can make accurate predictions. Figure 7(a) presents the five-layer inference structure of the model constructed by ANFIS. Figure 7(b) shows a 3D model view with the axial parameter adjusted to show the relationship between input and output values. Figure 7(c) shows the FIS model after training.

After constructing the FIS for each rotation speed for ANFIS, *i.e.*, after the predictive model of the control system is established, Simulink is used for the control and predictive analysis of the simulation system. The architecture of the simulation control and predictive analysis system is shown in Fig. 7(d).

The predictive analysis process of the analog control system is as follows:

1. Select one of the spindle rotation speeds and randomly select the following five input parameters of the speed as the operating state of the MT: thermal deformation in Z-direction,

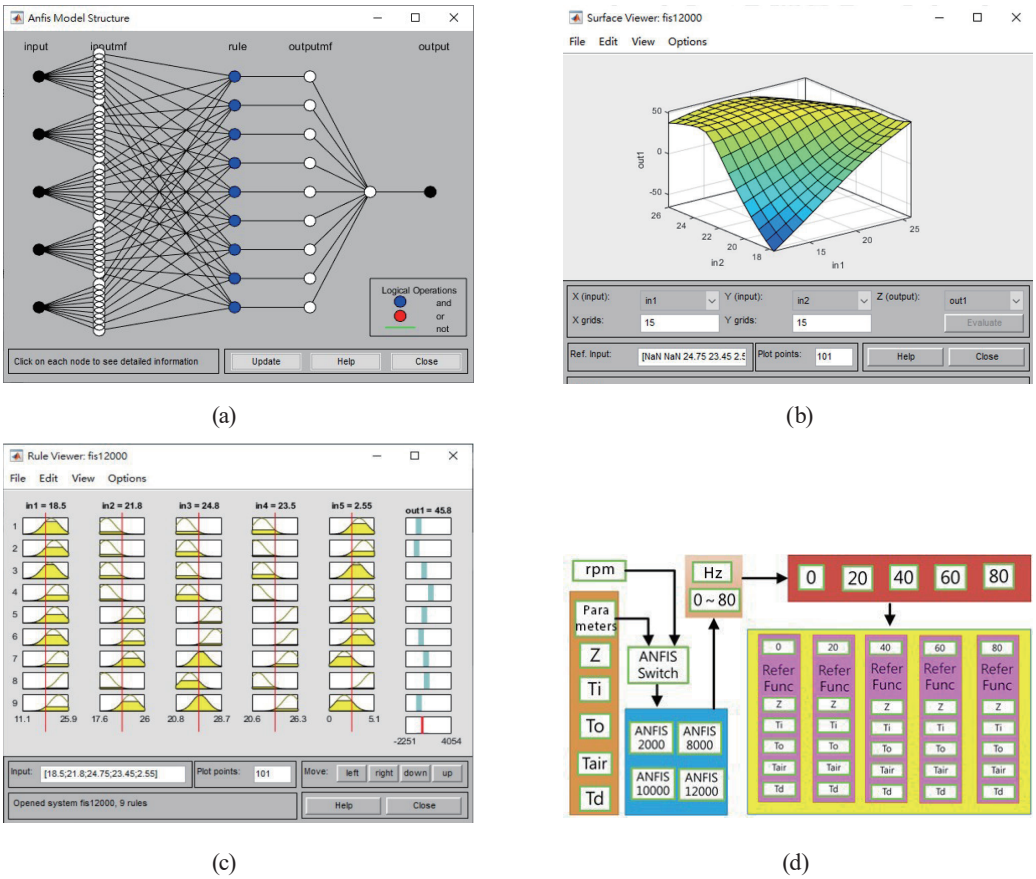

Fig. 7. (Color online) (a) Schematic of model structure, (b) 3D view of the model, (c) fuzzy rule inspection view, and (d) architecture of analog control and predictive analysis system.

inlet and outlet coolants temperatures, air temperature, and inlet and outlet coolants temperature difference.

2. The analog control and predictive analysis system first determines the spindle rotation speed, assigns the signal to the corresponding ANFIS for behavior prediction, and waits for the ANFIS of each rotation speed to analyze the coolant pump operating frequency.
3. After the ANFIS analysis is completed, the output of the coolant pump frequency is referred to as the curve-fitted data by decompiling the coolant pump frequency as a value for predicting the trend of the temperature and displacement changes in the main spindle. To predict the spindle speed and adjust the coolant pump frequency, the relevant data up to this frequency can be used to adjust the MT once the user knows the thermal restraint and predicts the thermal deformation of the spindle.

The above method is developed and implemented for the cooling control prediction for this study. The detected parameters of the spindle state are the initial input to the prediction system; after prediction, they can be used as the basis for the optimal adjustment of parameters after decompilation into the relevant parameters of the spindle state.

Figure 8 shows the frequency, temperature difference, and deformation relationship of the MT spindle. The temperature difference between the inlet and outlet coolants increases with increasing coolant pump frequency, and the deformation also increases with the coolant temperature difference.

The prediction system in this study uses MATLAB Simulink to obtain the expected system operation from the actual operation of the machine. The real test cannot quickly correct the accuracy and parameters of the prediction model in a short time because of the large amount of data. The use of software digital simulation to verify the performance of methods can reduce costs and generate data in various scenarios for testing. Therefore, Simulink was used in this study to operate the simulation control and predictive system to generate the data required for predictive analysis.

Table 2 shows the finally constructed relevant parameters of ANFIS for each rotation speed used in the Simulink simulation control and prediction system. Figure 9 shows the flow chart of the Simulink simulation control and prediction system. Figure 10 shows the main interface of the analog control and prediction system. The upper left corner of Fig. 10 determines the spindle speed and the lower-left corner determines the initial parameters of the spindle: thermal deformation in Z-direction, inlet coolant temperature, outlet coolant temperature, air temperature, and temperature difference between inlet and outlet coolants. The middle part is the ANFIS corresponding to the four speeds, and the right half gives the system prediction results.

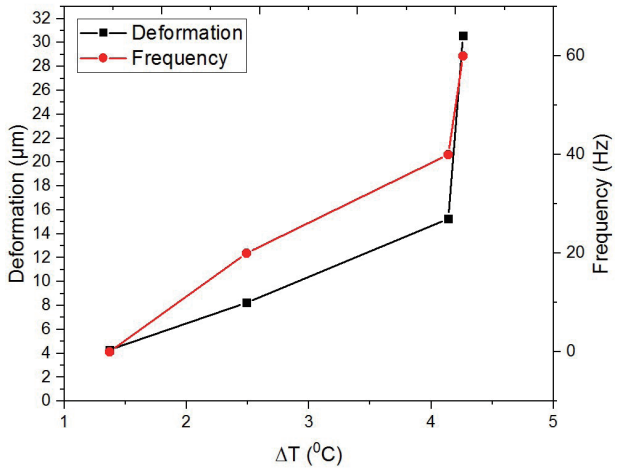

Fig. 8. (Color online) Frequency, temperature difference, and deformation relationship.

Table 2
Final ANFIS model used in prediction system.

ANFIS category	FIS generation method	Number of rules	Learning method	RMSE	R^2
2000	GP	2	Hybrid	5.365549	0.9044
8000	GP	2	Hybrid	3.838200	0.7419
10000	GP	2	Hybrid	3.776320	0.6800
12000	GP	2	Hybrid	5.453666	0.8447

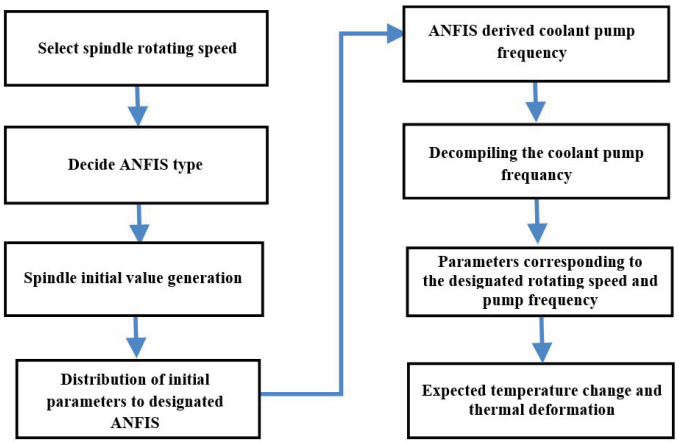

Fig. 9. (Color online) Flow chart of Simulink simulation control and prediction system.

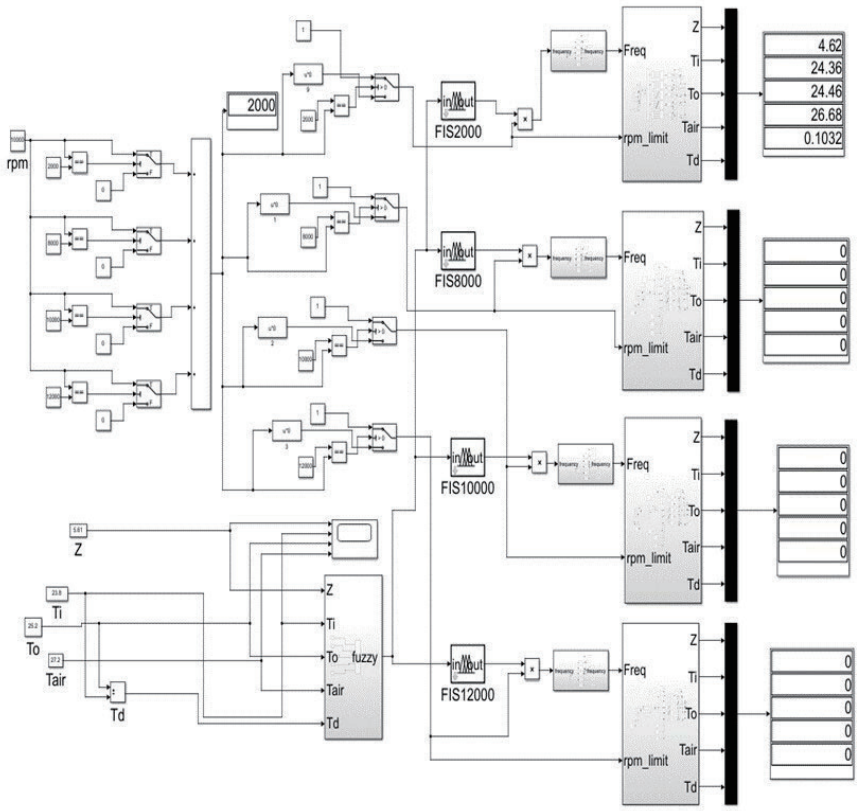

Fig. 10. Main interface of Simulink simulation control and prediction system.

3. Results and Discussion

In addition to finding that increasing the number of data should reduce the recording frequency of repeated data, we found from the data collation before establishing the model that

unsteady data are linearly fitted to identify the reliability of the recorded data. Linear polynomials can identify the changing trend of the data; thus, we use the Curve Fitting Toolbox in MATLAB to identify the changing trend of the data, and we determine the frequency of each spindle speed before fitting. All the steady-state interval data are input into the toolbox, and the changing trend of the data is fitted to a curve to generate the reference equation. Fourier transform (FT) is used to perform most curve fitting operations.

3.1 Regulation of model construction methods

By building the predictive model, we found that in ANFIS, for both the GP and SC methods, the type and complexity of the training data will directly affect the timing of using these methods, especially when the time series is used in the last stage. It is found that even if the same inference method is used, the same number of membership function rules of the FIS generated by the GP method and the FIS calculated by the SC method are used to generate the model and compare the RMSE. The results are nearly the same for the GP and SC methods. The RMSE used in the model construction has a significant reference value that can be used as an evaluation index. Although the RMSE value is a reference index for one of the mathematical models, it is based on the same type of data, and the evaluation index is calculated as a relative value. It is difficult to arbitrarily determine the efficiency of the model, and the practicability of the model must be determined through the actual implementation into the system and by observing the prediction status of the model.

3.2 Predicted results of control system

The cooling pump frequency deduced by the predictive model in the analog control system is converted using the data recorded during the steady-state interval for each spindle rotation speed as a reference. In ANFIS, one set corresponds to five frequency classifications. The best reference value after frequency conversion is predicted by the system.

Table 3 shows the frequency reference values predicted at 2000 rpm and the predicted cooling pump frequencies deduced by ANFIS in the analog control system for frequencies of 0, 20, 40, 60, and 80 Hz. Then the frequency reference values use the measurement data recorded in the study to take the steady-state interval as the best reference value.

From Table 3, when the spindle speed is 2000 rpm and the coolant pump operating frequency is set to 20 Hz, the input and output coolant temperatures of the spindle are 23.56 and 24.93 ℃, respectively. The temperature difference between the inlet and outlet coolants is 1.37 °C, which

Table 3
Predicted frequency reference values for spindle rotation speed of 2000 rpm.

Frequency (Hz)	Z (μm)	T_i (℃)	T_o (℃)	T_{air} (℃)	T_d (℃)
0	4.62	24.36	24.46	26.68	0.10
20	4.29	23.56	24.93	26.92	1.37
40	5.04	23.84	24.19	26.81	0.35
60	5.39	23.84	24.43	26.80	0.59
80	5.77	23.88	24.29	27.10	0.41

is the greatest temperature difference between the inlet and outlet coolants at this speed. Thus, the user can adjust the operating frequency of the coolant pump to 20 Hz when the spindle is rotating at 2000 rpm. With the operating frequency of 20 Hz at 2000 rpm, the thermal suppression effect is greatest, and 92.4% of the total heat is eliminated from the spindle.

From Fig. 11(a), it can be seen that the greatest temperature difference is at the coolant pump frequency of 20 Hz. Thus, adjusting the coolant pump operating frequency to 20 Hz at 2000 rpm has the greatest thermal suppression effect.

From Table 4, when the spindle speed is 8000 rpm and the coolant pump operating frequency is set to 40 Hz, the input and output coolant temperatures of the spindle are 27.95 and 30.44 °C, respectively. The temperature difference between the inlet and outlet coolants is 2.49 °C, which is the greatest temperature difference between the inlet and outlet coolants at this speed. Thus, the user can adjust the operating frequency of the coolant pump to 40 Hz when the spindle is rotating at 8000 rpm. At 40 Hz, its thermal suppression effect is the greatest, eliminating 99.9% of the total heat of the spindle. It is also observed that if the coolant pump frequency is adjusted to 80 Hz, the inlet coolant temperature is higher than the outlet coolant temperature. It is inferred that, for an operating frequency of 80 Hz, heat dissipation from the coolant to the ambient appears and the cooling effect for the spindle is rather weak.

From Fig. 11(b), it can be seen that the greatest temperature difference is at a coolant pump frequency of 40 Hz. Thus, adjusting the coolant pump operating frequency to 40 Hz at 8000 rpm has the greatest thermal suppression effect.

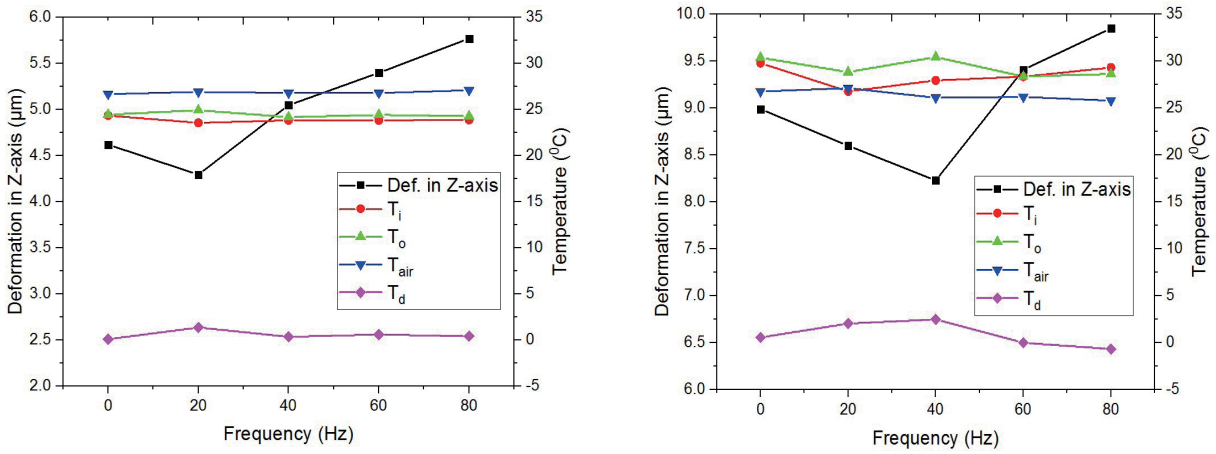

Fig. 11. (Color online) Predicted frequency reference values at a speed: (a) 2000 and (b) 8000 rpm.

Table 4
Predicted frequency reference values for spindle rotation speed of 8000 rpm.

Frequency (Hz)	Z (μm)	T_i (°C)	T_o (°C)	T_{air} (°C)	T_d (°C)
0	8.99	29.80	30.37	26.78	0.56
20	8.60	26.78	28.83	27.13	2.05
40	8.23	27.95	30.44	26.11	2.49
60	9.41	28.35	28.36	26.19	0.01
80	9.85	29.32	28.64	25.8	−0.67

From Table 5, when the spindle speed is 10000 rpm and the coolant pump operating frequency is set to 40 Hz, the input and output coolant temperatures of the spindle are 24.09 and 28.23 °C, respectively. The temperature difference is 4.14 °C, which is the greatest temperature difference between the inlet and outlet coolants at this speed. Thus, the user can adjust the operating frequency of the coolant pump to 40 Hz when the spindle is rotating at 10000 rpm. With the operating frequency of 40 Hz at 10000 rpm, the thermal suppression effect is greatest, and 80.1% of the total heat of the spindle is eliminated.

From Fig. 12(a), it can be seen that the greatest temperature difference is at the coolant pump frequency of 40 Hz. Thus, adjusting the operating frequency of the coolant pump to 40 Hz at 10000 rpm has the greatest thermal suppression effect.

From Table 6, when the spindle speed is 12000 rpm and the coolant pump operating frequency is set to 60 Hz, the input and output coolant temperatures of the spindle are 24.22 and 28.38 °C, respectively. The temperature difference between the inlet and outlet coolants is 4.16 °C, which is the greatest temperature difference between the inlet and outlet coolants at this speed. Thus, the user can adjust the operating frequency of the coolant pump to 60 Hz when the spindle is rotating at 12000 rpm. With the operating frequency of 60 Hz at 12000 rpm, its thermal suppression effect is the greatest, and 60.2% of the total heat of the spindle is eliminated.

Table 5
Predicted frequency reference values for spindle rotation speed of 10000 rpm.

Frequency (Hz)	Z (μm)	T_i (°C)	T_o (°C)	T_{air} (°C)	T_d (°C)
0	17.47	19.27	22.59	24.43	3.32
20	16.44	21.02	24.54	23.8	3.52
40	15.25	24.09	28.23	28.20	4.14
60	18.38	18.41	22.48	24.55	4.06
80	19.31	19.08	22.46	24.49	3.38

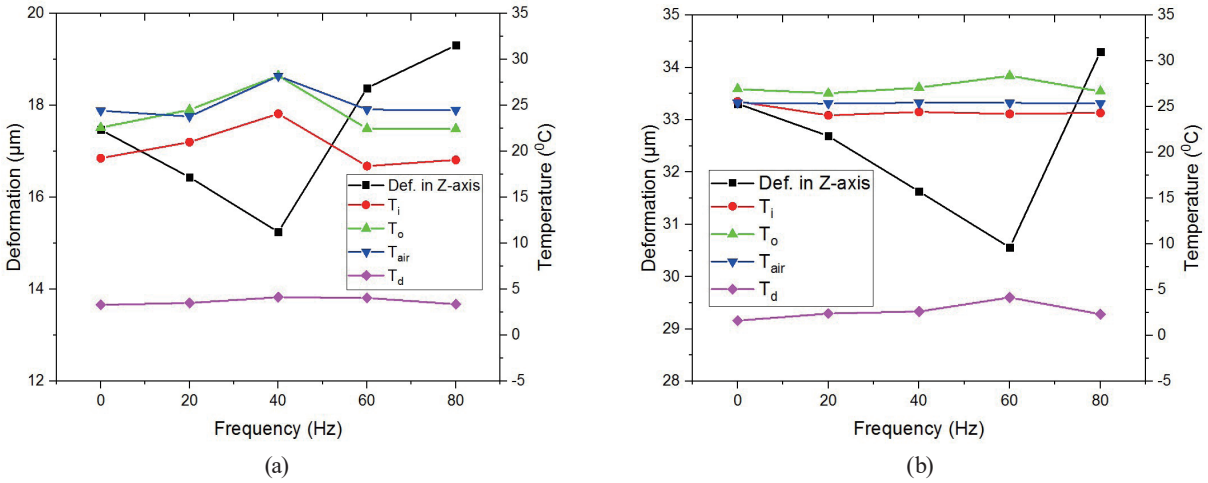

Fig. 12. (Color online) Predicted frequency reference values at a speed: (a) 10000 and (b) 12000 rpm.

Table 6
Predicted frequency reference values for spindle rotation speed of 12000 rpm.

Frequency (Hz)	Z (μm)	T_i (°C)	T_o (°C)	T_{air} (°C)	T_d (°C)
0	33.31	25.58	26.92	25.42	1.64
20	32.69	24.06	26.47	25.35	2.40
40	31.63	24.44	27.08	25.44	2.64
60	30.56	24.22	28.38	25.42	4.16
80	34.30	24.33	26.67	25.36	2.34

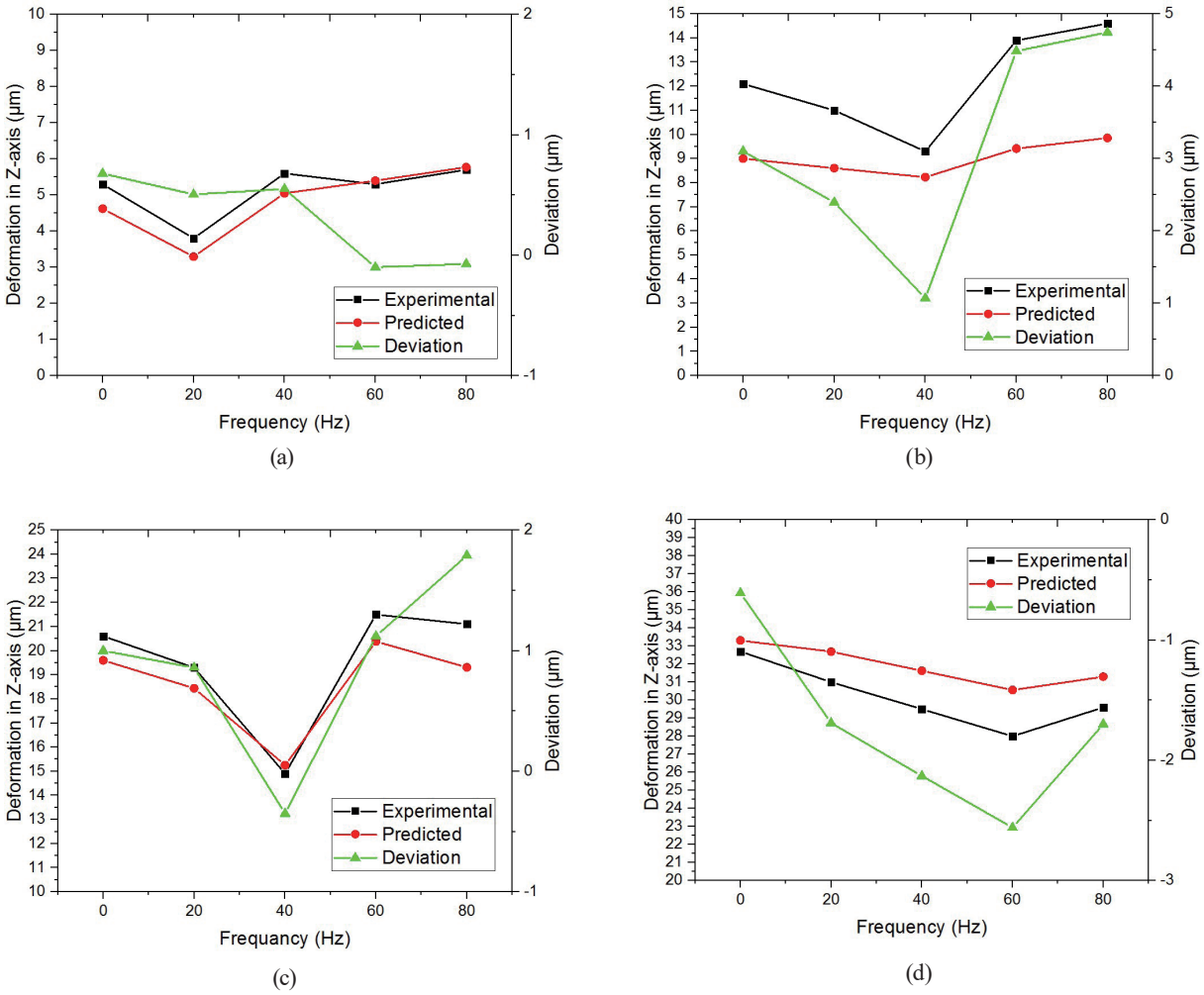

Fig. 13. (Color online) Deviation between experimental and predicted deformations in Z-direction: (a) 2000; (b) 8000; (c) 10000, and (d) 12000 rpm.

From Fig. 12(b), it can be seen that the greatest temperature difference is at the coolant pump frequency of 60 Hz. Thus, adjusting the operating frequency of the coolant pump to 60 Hz at 12000 rpm has the greatest thermal suppression effect.

Figure 13 illustrates the deviation between the experimental and predicted thermal deformations in the Z-direction. The thermal deformation predicted by this model is highly

accurate at different spindle speeds, and the deviation is within the ranges of −0.099 to 0.679 μm at 2000 rpm, 1.069 to 4.745 μm at 8000 rpm, −0.35 to 1.79 μm at 10000 rpm, and −2.56 to −0.60 μm at 12000 rpm.

4. Conclusions

In this study, the thermal suppression method is used to reduce the influence of the thermal deformation effect, and ANFIS is used as a cooling control method to predict the change in the thermal state of the spindle at a given rotation speed. The GP and SC methods are used for inference in ANFIS. The hybrid and BP learning methods are used to carry out the network calculation of ANFIS. The above methods are combined for predictive modeling, and RMSE is used to evaluate the performance of the model to determine the learning conditions of the model giving the best prediction. Finally, the model in Simulink is used to simulate the control and prediction system to determine the optimal coolant pump operating frequency at the specified spindle speed and thermal state to achieve the greatest thermal suppression effect.

The experimental results establish that the predictive model developed by the ANFIS control method is very efficient with prediction accuracy within 4.745 μm, and the simulation test also shows the feasibility of this method. The expected cost reduction and the accurate prediction of changes in the thermal state of the MT spindle indicate that this control method is feasible for the prediction and thermal suppression of MT spindles. The most suitable coolant pump frequencies at spindle speeds of 2000, 8000, 10000, and 12000 rpm to achieve the greatest spindle thermal suppression of the spindle are summarized below:

1. At a spindle speed of 2000 rpm, the coolant pump frequency should be adjusted to 20 Hz, which can reduce the total heat of the spindle by 92.4%.
2. At a spindle speed of 8000 rpm, the coolant pump frequency should be adjusted to 40 Hz, which can reduce the total heat of the spindle by 99.9%.
3. At a spindle speed of 10000 rpm, the coolant pump frequency should be adjusted to 40 Hz, which can reduce the total heat of the spindle by 80.1%.
4. At a spindle speed of 12000 rpm, the coolant pump frequency should be adjusted to 60 Hz, which can reduce the total heat of the spindle by 60.2%.

Acknowledgments

This research was funded by the Ministry of Science and Technology, Taiwan under Grant No. MOST 109–2622-E167–015 and 110-2622-8-167-002-TE5.

References

1 K. Y. Li, W. J. Luo, J. Z. Huang, Y. C. Chan, Pratikto, and D. Faridah: Appl. Sci. **7**, (2017) 420. https://doi.org/10.3390/app7040420
2 C. Zhang, F. Gao, and Y. Li: Precis. Eng. **47** (2017) 231. http://dx.doi.org/10.1016/j.precisioneng.2016.08.008
3 K. Y. Li, W. J. Luo, M. H. Yang, X. H. Hog, S. J. Luo, and C. N Chen: J. Mech. **35** (2019) 887. https://doi.org/10.1017/jmech.2019.29
4 K. Y. Li, W. J. Luo, and S. J. Wei: Appl. Sci. **10** (2020) 3991. https://doi.org/10.3390/app10113991

5 K. Y. Li, W. J. Luo, Y. Zeng, and I. Huang: Sens. Mater. **32** (2019) 3689. https://doi.org/10.18494/SAM.2020.3104
6 K. Y. Li, W. J. Luo, X. H. Hong, S. J. Wei, and P. H. Tai: IEEE Access **8** (2020) 28988. https://doi.org/10.1109/ACCESS.2020.2972580
7 S. N. Grama, A. Mathur, and A. N. Badhe: Int. J. Mach. Tools Manuf., **112** (2018) 3. https://doi.org/10.1016/j.ijmachtools.2018.04.004
8 T. Liu, W. Gao, Y. Tian, H. Zhang, W. Chang, K. Mao, and D. Zhang: Appl. Therm. Eng. **76** (2015) 54. http://dx.doi.org/10.1016/j.applthermaleng.2014.10.088
9 Y. Zhang, T. Liu, W. Gao, Y. Tian, X. Qi, P. Wang, and D. Zhang: Appl. Therm. Eng. **134** (2018) 460. https://doi.org/10.1016/j.applthermaleng.2018.02.016
10 W. M. Chiang, W. J. Luo, and F. J. Wang: J. Mech. Sci. Technol. **32** (2018) 1391. https://doi.org/10.1007/s12206–018–0242–5
11 K. Mori, B. Bergmann, D. Kono, B. Denkena, and A. Matsubara: CIRP J. Manuf. Sci. Technol. **25** (2019) 14. https://doi.org/10.1016/j.cirpj.2019.04.003
12 J.-S. R. Jang: IEEE Trans. Systems, Man, and Cybernetics **23** (1993) 665. https://doi.org/10.1109/21.256541
13 D. R. Keshwani, D. D. Jones, and R. M. Brand: Cutaneous and Ocular Toxicology **24** (2005) 149. https://doi.org/10.1080/15569520500278690
14 M. Al-Mahasneh, M. Aljarrah, T. Rababah, and M. Aludatt: Food Processing Reviews **8** (2016) 351. https://doi.org/10.1007/s12393-016-9141-7
15 A. Y. Sonmez, S. Kale, R. C. Ozdemir, and A. E. Kadak: Turk. J. Fish. Aquat. Sci. **18** (2018) 1333. http://doi.org/10.4194/1303-2712-v18_12_01
16 B. A. Bensaber, C. G. P. Diaz, and Y. Lahrouni: J. Comput. Sci. **47** (2020) 101234. https://doi.org/10.1016/j.jocs.2020.101234
17 E. Akkaya: Fuel **180** (2016) 687. http://dx.doi.org/10.1016/j.fuel.2016.04.112
18 A. M. Abdulshahed, A. P. Longstaff, and S. Fletcher: Appl. Soft Comput. **27** (2015) 158. http://dx.doi.org/10.1016/j.asoc.2014.11.012
19 E. Soroush, M. Mesbah, N. Hajilary, and M. Rezakazemi: J. Environ. Chem. Eng. **7** (2019) 102925. https://doi.org/10.1016/j.jece.2019.102925
20 S. O. Sada and S. C. Ikpeseni: Heliyon **1** (2021) e06136. https://doi.org/10.1016/j.heliyon.2021.e06136
21 S. G. Milan, A. Roozbahani, N. A. Azar, and S. Javadi: J. Hydrol. **598** (2021) 126258. https://doi.org/10.1016/j.jhydrol.2021.126258

About the Authors

Ming-Chu Hsieh received her Ph.D. degree from National Taiwan University of Science and Technology in 2013. She is currently an associate professor in the Department of Mechanical Engineering at National Chin-Yi University of Technology, Taichung County, Taiwan. Her research interests are in computer-aided design, reverse engineering, mechanical design, industrial design, and product innovation design. (smj@ncut.edu.tw)

Swami Nath Maurya received his B. Tech degree from the Department of Instrumentation and Control Engineering, Bundelkhand University (BU), Jhansi, India, in 2011 and his M. Tech degree from the Department of Green Energy Technology, Pondicherry University (PU), Puducherry, India, in 2015. He spent more than six years working in different Indian solar industries. He is currently pursuing a Ph.D. degree from the Graduate Institute of Precision Manufacturing, National Chin-Yi University of Technology, Taiwan. His research interests include thermal errors of machine tools, solar energy, renewable energy, energy saving, sensors, and artificial intelligence. (smaurya077@gmail.com)

Win-Jet Luo received his Master's degree in engineering in 1994 and his Ph.D. degree in engineering in 2000 from National Chen Kung University, Taiwan. He is a distinguished professor at the Graduate Institute of Precision Manufacturing, National Chin-Yi University of Technology, Taiwan. His research has mainly focused on computational fluid dynamics, microelectromechanical systems, ventilation, energy saving, fuel cells, and microsensors. He has published several research papers in prestigious international journals and has been invited to review journals. (wjluo@ncut.edu.tw)

Kun-Ying Li was born in Chiayi, Taiwan, in 1979. He was an engineer with the Intelligent Machinery Technology Center, Industrial Technology Research Institute from 2007 to 2020. He received his Ph.D. degree from National Chin-Yi University of Technology, Taiwan, in 2020. He has been an assistant professor since 2020. His research interests include thermal errors of machine tools, design for precision machinery, and reliability engineering and applications. He holds 14 patents in machine tools and has published many research papers in prestigious journals. (likunying@ncut.edu.tw)

Li Hao received his Master's degree from the Department of Mechanical Engineering, National Chin-Yi University of Technology, Taichung, Taiwan, in 2020. His research interests are machine tools, artificial intelligence, MEMS, bio-engineering, and sensors. (geasslee@gmail.com)

Prakash Murgeppa Bhuyar received his Ph.D. degree in industrial biotechnology from Universiti Malaysia Pahang, Malaysia, and is currently working as a lecturer at International College (MJU-IC), Maejo University, Thailand. His research interests are algae, biotechnology, biofuel, renewable energy, molecular biology, and wastewater management. (prakash@mju.ac.th)